Quantification of Bioaccessible and Environmentally Relevant Trace Metals in Structure Ash from a Wildland Urban Interface Fire

Carmen M. Villarruel[1], Linda A. Figueroa[2], James F. Ranville[1*]

[1]Department of Chemistry, Colorado School of Mines, Golden, CO, 80401; cvillarruel@mines.edu (C.M.V.); jranvill@mines.edu (J.F.R.);
[2]Department of Civil and Environmental Engineering, Colorado School of Mines, Golden, CO, 80401; lfiguero@mines.edu

Abstract. Wildfires at the Wildland Urban Interface (WUI) are increasing in frequency and intensity, driven by climate change and anthropogenic ignitions. Few studies have characterized the variability in metal content in ash generated from burned structures in order to determine potential risk to human and environmental health. Using Inductively Coupled Plasma Optical Emission Spectroscopy (ICP-OES) and Inductively Coupled Plasma Mass Spectrometry (ICP-MS) we analyzed leachable trace metal concentration in soils and ash from structures burned by the Marshall Fire, a WUI fire that destroyed over 1000 structures in Boulder County Colorado. Acid digestion revealed that ash derived from structures contained 22 times more Cu and 3 times more Pb on average than surrounding soils on a mg/kg basis. Ash liberated 12 times more Ni (mg/kg) and twice as much Cr (mg/kg) as soils in a water leach. By comparing the amount of acid-extractable metals to that released by water and Simulated Epithelial Lung Fluid (SELF), we estimated their potential for environmental mobility and human bioaccessibility. The SELF leach showed that Cu and Ni were more bioaccessible (mg leachable metal/mg acid extractable metal) in ash than in soils. These results suggest that structure ash is an important source of trace metals that can negatively impact the health of both humans and the environment.

Keywords: Wildfire, WUI, Simulated Epithelial Lung Fluid, ICP-MS, metal mobility

Synopsis: Wildfires at the Wildland Urban Interface burn metal containing structures, generating ash that may be hazardous to humans and the environment.

Introduction. Over the past three decades, fire season in the United States has become more severe as the annual number of fires and area burned increases[1–5]. This increase has been largely driven by climate change[3,6–10]. The average wildfire size has increased 4-fold during the 2000's[11] as compared to the previous 2 decades. In 2022 alone, 7.4 million acres were burned by nearly 65,000 fires[12,13]. The increase in wildfire size and frequency in the US has coincided with the expansion of the Wildland Urban Interface (WUI), a region where houses and structures are interspersed among vegetation and forests[14–16]. Close proximity of vegetative fuel to structures elevates the risk of fire propagation, increasing WUI susceptibility to burning[15,17,18]. As of 2021, there were approximately 50 million US homes in the WUI, with an expected increase of 1 million within 3 years[19]. From 1990 to 2010, the WUI grew by 41% in the US[18], accounting for approximately 39% of all houses[14,17] and 10% of land area[15]. Between 1985 and 2013, approximately 69% of structures destroyed in wildfires existed in the WUI[17]. The destruction of structures at the WUI due to wildfires is a problem that is expected to increase as more people move into the WUI, and climate change continues to progress, increasing wildfire activity[20].

Wildfires have a direct impact on air quality. Wildfire smoke contains volatile organic molecules, fine particulate matter ($PM_{2.5}$, PM_{10}), ozone, aldehydes, sulfur dioxides, and other contaminants[21–24] which have been linked to increases in overall mortality and respiratory morbidity[25–32]. Hospital admissions increase during wildfire activity[31,33,34] with respiratory admissions increasing 23-34%[28,35,36]. Repeated annual exposure carries additional risk of long-term illness including elevated risk for developing lung cancer or brain tumors[37]. Wildfires also impact environmental health by destroying vegetation[38,39], altering animal behavior[40], and generating ash and atmospheric particulates. Following severe burns, slopes lose the vegetation that prevents erosion[41], increasing vulnerability to debris flow landslides during

rainstorms[42]. Erosion and wind events deposit ash onto soils[43–45] and surface waters[46–51], thus contaminating water sources[52,53] and increasing sediment load[54].

Wildfire ash and burned soils are often enriched in trace metals[43,55,56]. Metals can become volatilized at high temperatures during combustion and then condense, subsequently adsorbing to ash surfaces during cooling[44,45]. Studies have also shown that the conditions present during combustion can induce transformations in metal speciation across matrices including soils, coal, and biomass[57–61]. These alterations to metal speciation can increase the mobility and toxicity of metals[57,58,60], underpinning the urgency for quantification in environmental systems. Trace metal concentration in ash is highly dependent on the metal content[43,56] and overall composition of the burned materials[45,51,62,63]. For example, electronics in the built environment contain metals such as Cd, Cr, Ni, Pb, and Zn in high concentrations[64–66]. These electronics require proper disposal to prevent contamination of soils and water. Currently, few studies have focused on metal concentrations in ash from WUI fires[67–70], which often burn electronics in structures.

The Marshall Fire, a WUI fire in Boulder County, was the most destructive fire in Colorado history. Over the course of 2 days, the Marshall Fire destroyed 1084 structures, primarily residential dwellings, and burned over 24 square kilometers. In contrast to wildfires, which burn mostly vegetation, structures are highly concentrated sources of bulk metals, which are present in structural components such as support beams (Ni and Cr in steel), plumbing (Cu and Pb), wiring (Cu), electronics (Cu, Ni, Pb, Cr), and paint (Cr, Cu, Pb). Nevertheless, exactly how the presence of bulk metals in materials subjected to WUI fires impact final metal concentration in ash is poorly understood. To date, there has been little research to determine the composition of ash generated from burned structures, and its potential for environmentally and biologically relevant metal release.

Rapid expansion of WUI[18,71] and increase in wildfire activity[12,18,72] will lead to increased quantities of structure ash, and it is imperative to understand the impacts that this may have on human and environmental health. Metal mobilization is of environmental concern due to the persistence, mobility, bioavailability, and bioaccumulative properties of trace metals[43,63] which can be examined through the use of laboratory-based extraction procedures. The purpose of this study was to determine the identity and concentration of metals in ash generated from the Marshall Fire. Specifically, we examined situationally relevant matrices such as water and Simulated Epithelial Lung Fluid (SELF) to assess the metal leaching potential of ash produced by structural fires. In the WUI, soil is an existing source of leachable metals and $PM_{2.5,10}$[73–75]. Therefore, we compared the metal concentrations and leaching behavior of ash to that of native soils in order to test the hypothesis that metals are elevated in the local environment as a result of ash from WUI structure fires post wildfire.

Materials and Methods

Sampling. The Marshall fire burned December 30-31, 2021. Ash and surficial soil samples were collected 3 months post fire (March 2022). Prior to sampling, 3.77 inches of new precipitation in the form of snow was recorded[76]. Some of this snow melted and sublimated in place, and freezing temperatures primarily occurred prior to sampling, suggesting that leaching of metals prior to collection was limited. Four locations were examined within the Marshall fire perimeter (approximate sampling locations shown in Figure S1). At the western-most site (S1) a large number of individual samples (n = 31) were collected across a residential property in order to examine the spatial variability in metal content within the burned structure and the surrounding soils. Each sample was comprised of multiple collections of specific material (ash or soil) from the immediate sample location. At the other sites (S2 – S4) we created single composites from multiple individual locations to obtain an average composition for each entire site.

Workers clearing the S1 site had piled and homogenized ash in one location, which we also sampled as the S1 composite. Samples were categorized as ash or soil, according to information obtained from homeowners, visual inspection of the material, and the sampling location within the site. Soil samples (n=8) included burned and unburned soils that were separate from the burned structure. Ash samples (n= 23) included ash collected from throughout the structure, burned landscape lumber, and burned material that likely orignially contained electronics (as per personal communication with homeowner). Samples were collected by steel trowel, placed in polyethylene zipper closable bags, and dried at ambient room temperature in the laboratory. A portion of each sample was sieved with a No. 10 mesh stainless steel screen, and the resulting <2 mm portion was carried forward in the subsequent analysis. Dry samples were stored at 4 °C until analysis. With these procedures, that are based on the USGS methodology to sample metal-rich solid wastes[77], we obtained a representative average concentration, but did not determine uncertainty in subsampling. Given each sample was a composite of many individual collections, and the sieving process both homogenized the sample and rejected large particles, leaching and analysis was performed on single subsamples.

Acid Leachable Metals. Acid recoverable metals in ash and soil samples were extracted using a modified EPA method designed for solid waste materials[78–80], which is expected to liberate mobile, environmentally relevant metals. Approximately 200-300 mg of ash or soil were transferred to 15 ml Falcon polypropylene tubes (VWR). We added 0.6 mL of nitric acid (Macron, Optima Grade), that was previously diluted 50:50 with deionized water (18 MΩ·cm, Nanopure). Then 0.3 ml of hydrochloric acid (Fisher Chemical, Optima Grade), diluted 50:50 with deionized water, was added. Samples were digested overnight at room temperature. Subsequently, 10 ml of Nanopure water was added gravimetrically. Uncapped tubes were evaporated at 83 °C until the volume was reduced to approximately 2 ml. Samples were inverted to homogenize, lightly re-capped, and heated for 30 minutes to bring internal temperature to approximately 95 °C. Samples were cooled and total volume was brought to 10 ml with deionized water gravimetrically. Remaining solids were allowed to settle overnight. Samples were then filtered with a 0.45 µm nylon filter (Agilent 25 mm), diluted with MΩ·cm water and adjusted to 2% nitric acid (Trace metal grade, Fisher Chemical) for metals analysis by ICP-OES (PerkinElmer Optima 8300) and ICP-MS (PerkinElmer NexIon 300D). Method blanks (Nanopure) were included in the leaching procedure and all results. All method blanks were below the analytical limit of detection (mean + 3 SD of replicate QA blanks) for the elements analyzed.

Water Leach for Environmentally Labile Metals. A modified USGS method was used[77]. 0.5 grams of sample were transferred to a 15 ml Falcon tube and 10 g of 18 MΩ·cm water was added gravimetrically to each tube. Samples were vortexed for 5 seconds, leached at room temperature for 24 hours, and filtered with a 0.45 µm nylon filter (Agilent 25 mm). Samples were diluted with Nanopure water, adjusted to 2% nitric acid (analytical grade, Fisher Chemical), and analyzed via ICP-OES (PerkinElmer Optima 8300) and ICP-MS (PerkinElmer NexIon 300D).

Simulated Epithelial Lung Fluid (SELF) Leach. A modified Gamble's solution developed by Boisa et al[75] was selected as it included the major components of epithelial lung fluid, including salts, proteins, and organic acids. We excluded dipalmitoyl phosphatidyl choline (DPPC) as it has little impact on metal bioaccessability[81,82]. We used 20 ml of SELF based on the approximate lung volume in an adult human[75,81,82], and a 1:100 solid: SELF ratio was selected[74,82,83].

The inorganic components (SI Table 1) of SELF were dissolved in 500 ml of 18 MΩ·cm water in a 1-L High-Density Polyethylene bottle. Separately, the organic components (SI Table 1) were dissolved in 500 ml of Nanopure water. The two solutions were combined for a total solution volume of 1L. The protein and amino acid components were added as dry solids. The SELF was homogenized by shaking, and pH

was adjusted to 7.4 ±0.2 using HCl (Fisher Chemical). Sodium Chloride and Calcium Chloride, Ascorbic Acid, Uric Acid, Glycine, and Cystine were obtained from Fisher Chemical. Sodium Phosphate dibasic, and mucin from porcine stomach (type III) were obtained from Sigma-Aldrich. Sodium Bicarbonate, USP grade, was purchased from Baker Chemicals. Sodium sulphate and albumin from bovine serum were purchased from Oakwood Chemical. Glutathione was obtained from Acros Organics. Potassium chloride was obtained from Mallinckrodt Chemicals, and Magnesium Chloride was purchased from Macron.

Approximately 200 mg of ash or soil was added to 50 ml Falcon tubes containing 20 ml of SELF. Samples were capped and incubated for 24 hours at 37 °C on an incubated orbital shaker (New Brunswick Scientific Incubator Shaker Series I26) operated at 30 RPM to simulate the dynamic environment of the lung. Although material may be trapped in the lung for longer than 24 hours, metal concentration in lung fluid stabilizes at 24 hours[82]. Samples were centrifuged at 4500 x g (Eppendorf centrifuge 5810) for 10 minutes, filtered through a 0.45 µm nylon filter (Agilent, 25 mm), diluted with water (Nanopure), and analyzed for metal content via ICP-OES (PerkinElmer Optima 8300) and ICP-MS (PerkinElmer NexIon 300D).

ICP-MS/OES Analysis. ICP-OES (PerkinElmer Optima 8300) was utilized to screen a broad suite of elements (SI table 3-5). Calibration curves were created from High Purity Standards (HPS) according to the EPA 200.7 methods[79]. An internal standard (Sc, SPEX) was continuously introduced during the analysis to monitor instrumental drift. Corrections were <5-10% and if drift exceeded 20%, the run was stopped and the instrument recalibrated. Check standards consisted of NIST 1643f, CCV nonmetals (HPS), and CCV metals (HPS) and were analyzed at the start of analysis, midway through the analysis, and after all samples had been analyzed.

Selected elements at low concentrations as determined by ICP-OES were analyzed by ICP-MS (PerkinElmer NexIon 300D) due to its higher sensitivity. Standard curves were created using a 3-point calibration made from dilution of a 10 µg/ml (VWR Aristar Multi element ICP-MS Standard). The isotopes used in analysis were ^{63}Cu, ^{52,53}Cr, ^{60}Ni, and ^{208}Pb. Process blanks (2% HNO_3) were run alongside samples, and all returned values were below both the instrumental Detection Limit (DL) and Limit of Quantification (LOQ).

Elemental masses in the leachate were normalized to mass of ash or soil used and reported as mg/kg. The mass of solid sample and volume of leachate were used to compute the LOQs after conversion to mass concentration (mg/kg) in the initial solid (see SI Equation 1). Instrument detection limits for ICP-OES and ICP-MS were calculated by running 3 to 10 blanks (2% acid) and setting the instrumental detection limit at 3 times the standard deviation above the average blank reading. Following the application of the instrument detection limit, a limit of quantification based on the mass of soil or ash was applied. Using the instrument detection limits and the mass of solid leached, the limit of quantification (LOQ) was established for each element and defined at 10 times the lowest estimate, according to equation 1 (SI Table 2-4).

Statistical Analysis. Relationships between the ash and soil samples for metal content were examined using MATLAB (9.11.0.1837725 (R2021b)). Sample data was non-normally distributed necessitating the use of nonparametric analysis, so a 2-sided Wilcoxon Rank Sum Test was used to test the null hypothesis that the two sample sets (ash and soil) were from the continuous distributions with equal medians against the alternate hypotheses that they were from distinct distributions. An alpha value of 0.05 was used in all statistical analysis.

Linear correlations among leachable metal concentrations were explored using the Pearson's Correlation Coefficient (r) (Figure S4-7). A Pearson's correlation coefficient (r) of 0.75 was selected as a criterion to

state samples have a strong correlation. Only samples with a statistically significant correlation ($p < 0.05$) are reported.

Results and Discussion

Acid-Extractable Metal Concentrations

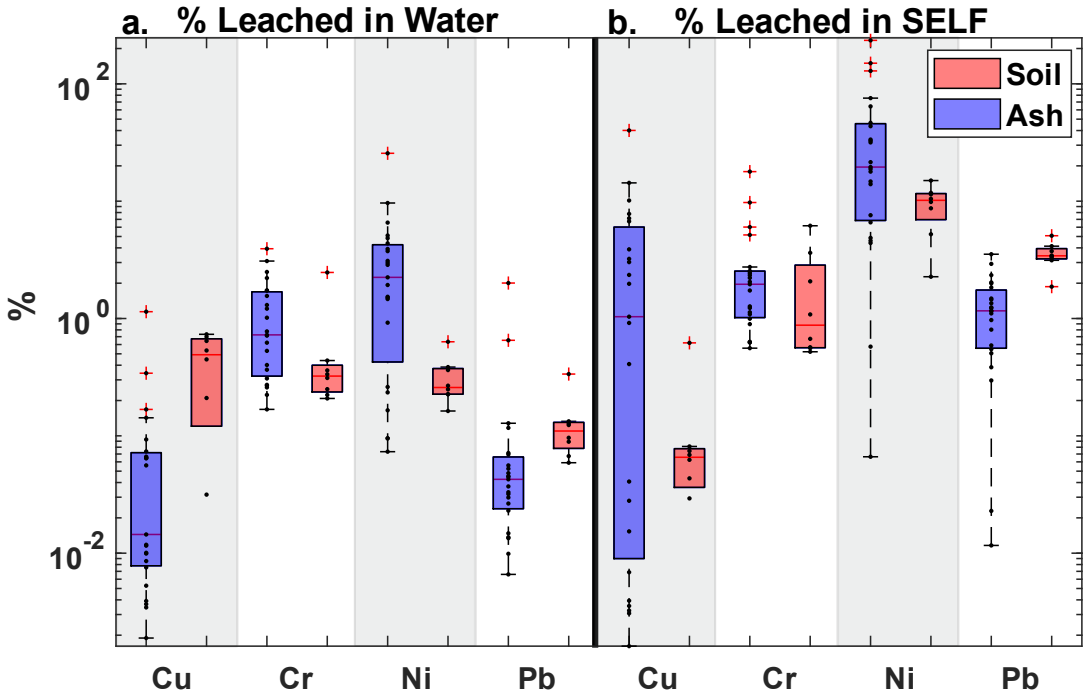

Figure 1. Box and whisker plot for trace metal concentrations (mg/kg) that were liberated by (a) acid and (b) deionized water. Individual data points are marked with black dots and the outliers (samples >1.5 times the interquartile range away from the bottom or top of the box) are shown as a red "+". The median, 25th and 75th percentiles are shown by the box. Whiskers indicate data spread, excluding outliers. n=8 for soil samples, n=23 for ash samples.

The concentrations of acid extractable trace metals (mg/kg) in ash and soil ranged over approximately 2 orders of magnitude (Figure 1a), with most variation most variation due to the range of acid labile Cu in ash Cu in ash. Smaller variations among Pb, Cr, and Ni concentration suggest higher uniformity in total metal across samples. Samples with metal concentrations below the DL (Table S-2-S4) are reported as the Limit of Quantification concentration. This conservative assumption provides an upper limit in concentration for the metals when present below the DL.

Ash samples were approximately 22 times higher in acid-leachable Cu compared to soil samples. This difference was statisically significant ($p = 3.4E-4$) and suggests that Cu in the residential structure contributed to the metal content of the ash. Cu concentrations in ash ranged from 19.3-4039 mg/kg with an average of 678 mg/kg. Data for Cu content in ash generated from wildfires that predominantly burned vegetation as reported in the literature is highly variable, with Cu concentrations ranging between 0.35-50 mg/kg[56,62], although one study found Cu concentrations of up to 15000 mg/kg in structure ash[68]. Soil Cu concentrations ranged from below the LOQ to a single outlier of 161 mg/kg. The average Cu

concentration in soils was 31 mg/kg, which is slightly elevated compared to both the 10.7-20.8 mg/kg reported for Colorado soils[84] and the global crustal abundance (GCA) of 14-28 mg/kg[85].

Cr concentrations ranged from 1.2-17.1 mg/kg with an average of 8.8 mg/kg in ash samples and from 1.2-13.8 mg/kg with an average of 9.5 mg/kg in the the soil samples. Mean Cr concentrations in both ash and soil were lower than the reported Colorado abundance (20-39 mg/kg)[84] and the GCA of 35-92 mg/kg[85]. This is likely due to the resitance of Cr metals to simple acid dissolution. No statistically-significant difference was found between the ash and soil Cr concentations ($p=0.44$), suggesting that, unlike Cu, the presence of this metal in the structure did not contribute significant amounts of acid leachable metal to the ash as compared to the surrounding soils.

Despite the fact that ash samples contained two Ni outliers with high concentration, there was no significant difference in average Ni concentration between the soil and ash samples ($p=0.58$). There was more spread in the the concentrations of Ni in ash, suggesting higher variability in ash than in the native soils. The concentration of Ni in ash samples was between 3.1-493 mg/kg with an average of 36 mg/kg, while soil samples ranged from 1.4-13.4 mg/kg with an average of 9.6 mg/kg. Ni in structure ash has been reported between approximately 0-350 mg/kg[68]. The average Ni concentration in soil is close to the lower end of that reported for Colorado soils (9.3-19.1 mg/kg)[84] and lower than the 19-47 mg/kg reported for the GCA[85].

Ash samples were significantly higher in Pb than soil samples ($p=0.036$). Pb concentrations in ash ranged between 0.4-142 mg/kg, aligning with median reported Pb concentrations of 350 mg/kg in structure ash[68]. Soil Pb ranged from 1.9-17 mg/kg. The average ash Pb sample was enriched nearly 3 times, at 29.1 mg/kg compared to the soil sample average of 9.1 mg/kg. The average Pb measured in soil is in general agreement with the Colorado soil average of 5.5-21.7 mg/kg[84], and lower than the GCA of 17 mg/kg[85].

Generally, the ash samples that were enriched in acid-extractable metals were associated with starting materials also elevated in those metals, informed by prior knowledge of the structure. This is especially evident in the outliers. The highest measured Ni concentration (493 mg/kg) was sampled from the location of a storage room that housed a large quantity of electronics (information provided by the homeowner). Nickel is used in electronics due to its high conductivity and low corrosivity. The ash sample containing the highest concentration of Pb was a composite of a house at S2 (Figure S1), composed of many different burned strucure materials. No specific information was obtained as to the contents of this house, however, Pb has historically been used in building materials, paints, and plumbing, especially in structures built before 1978[86]. Combustion of anthropogenic materials, specifically copper chromate arsenic (CCA) treated woods, has been linked to Cu accumulation on ash surface via a vaporization-condensation mechanism[69], which may account for some of the observed Cu enrichment as CCA wood was used in construction for structures prior to 2004[87]. Combustion of anthropogenic materials, specifically copper chromate arsenic (CCA) treated woods, has been linked to Cu accumulation on ash surface via a vaporization-condensation mechanism[69,87]. Reported Cu and Cr values from high temperature combustion of CCA treated wood range from 69-116 g kg^{-1} and 62-180 g kg^{-1} respectively, with As, Cu, and Cr accounting for 4-35% of total ash mass[67,69]. Lower concentrations and percent by mass of Cu and Cr in this study inhibit definitive identification of CCA woods and suggests higher heterogeneity of burned materials or lack of CCA treated wood in sampled structures. Indeed, none of the samples were collected where CCA-treated wood was likely used (i.e. landscaping) nor did any sampled materials have the appearance of burned CCA-treated wood. Some of the samples with high Cu concentrations were associated with ash sampled from the basement electronic room, consistent with the use of Cu in electronics. Enrichment of Pb in burned soils and ash post wildfire is highly dependent on burning temperature, with lower temperatures inducing Pb accumulation and higher temperatures (>600-

650 °C) leading to volatilization[43,55]. Structure fires burn at temperatures between 400-500 °C[88], suggesting that temperatures were inadequate for Pb volatilization and instead favored accumulation, which is supported by our measured concentrations. Ni and Cr form condensed species at temperatures higher than Pb or Cu[61]. The combustion temperature of the structure was likely not high enough to induce a vaporization-condensation mechanism for Ni and Cr, leading to retention in the ash fraction[43]. A recent analysis of structural and vehicle ash provides evidence that enrichment of some metals (Cr, Co, Cu, Ni, Zn) is observed compared to vegetation[68]. Although little work has been done to directly examine the mechanism of metal release from anthropogenic structure combustion, studies on wildfire ash and combustion of trace metal containing materials (i.e. BBQ coal [45]) show trace metal enrichment behavior in ash.

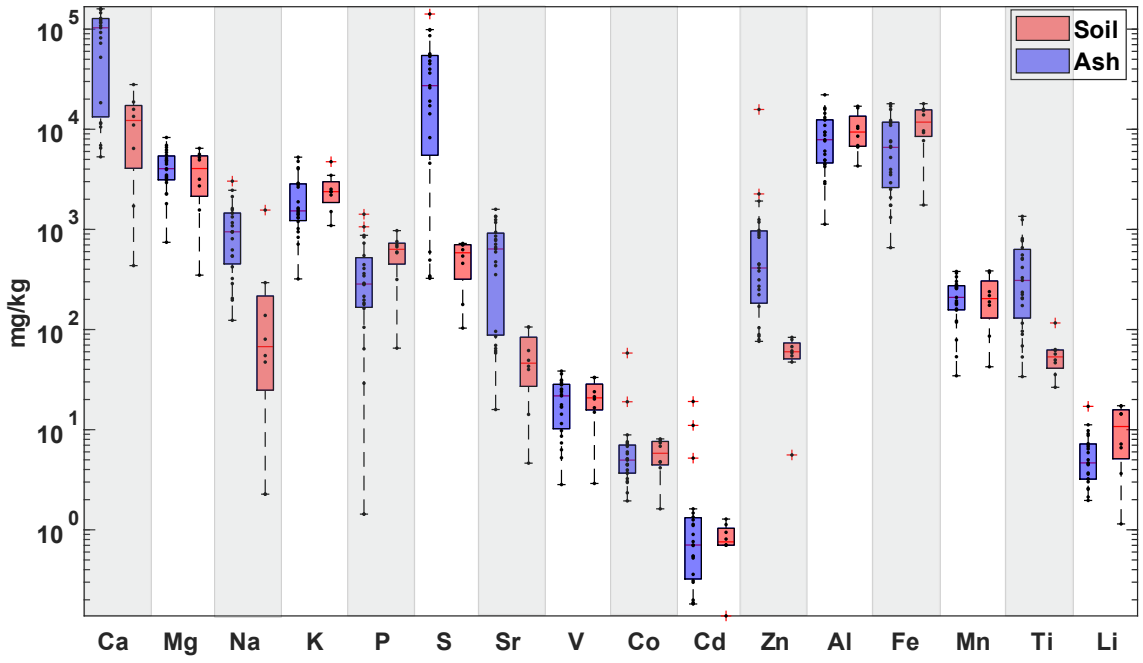

Figure 2. Box and whisker plot showing acid leachable oxide forming metals (Al, Fe, Mn, Ti, Li), major cations (Ca, Mg, Na, K), and trace metals (S, Sr, V, Co, Al, Fe, Mn, Ti, Li) (mg/kg) in ash (blue) and soils (red). Individual data points are marked with black dots and the outliers (samples >1.5 times the interquartile range away from the bottom or top of the box) are shown as a red "+". The median, 25th and 75th percentiles are shown by the box. Whiskers indicate data spread, excluding outliers. n=8 for soil samples, n=23 for ash samples.

Oxide forming metals (Al, Fe, Mn, Ti) were examined in the ash and soil samples (Figure 2). Differences between the ash and soil concentrations were only found for Ti. Ash samples, with an average of 424 mg/kg, have significantly higher concentrations of Ti than soil samples (p=5.5E-4), a trend reported in previous studies[68]. Ti comprises approximately 0.2% of Colorado soils[84], however we found Ti at much lower concentrations, with an average of 57 mg/kg, possibly due to incomplete acid digestion. Although structures contain Ti in paints, stainless steel, and electronics, a source has not been definitively identified. Higher Ti concentrations in ash corresponded to structure composites. Major cations (Ca, Mg, Na, K) were also examined in the ash and soil samples. We found that ash contained significantly higher concentrations of Ca and Na than soils, which has previously been reported in wildfire ash[47]. Ca and Na are major constituents of ash, especially at high combustion temperatures (>450C)[89]. Increased Ca in ash

have been reported in association with hydroxides and carbonates, contributing to the basicity of ash[90,91]. The ash samples were also found to be significantly higher in S and Sr ($p = 0.0036$ and 0.0012, respectively). The highest Sr concentrations were found in the electronics storage room samples and in the structure composites. The exact sources of Sr are not clear, although increased Sr concentration have been reported with increasing combustion completeness[68]. Enrichment of sulfur in ash has been reported in laboratory studies of burned biomass[92].

Knowledge of the home site provided by the homeowners aided in identification of some materials. One sample was identified as burned playground crumb rubber. The tire manufacturing process uses zinc for vulcanization at concentrations of 1-2%[93] and Cr at 0.0097%[94]. Zn comprised 1.58% and Cr at 0.0013% by mass in the sample. Results suggest that during combustion, zinc behaved conservatively, while Cr concentration was lower than expected based on literature values, suggesting that it may experience loss during combustion or was incompletely recovered during digestion. A second sample was suspected to be drywall, which is composed of 70-90% gypsum ($CaSO_4$) and cellulose. The exact composition of drywall varies between manufacturers, however gypsum contains 29.4% Ca and 23.6% S. We found that the acid leachable fractions in the suspected drywall contained 15.7% Ca and 14.2% S, a difference of 40.4-60.7%, which is attributed to incomplete digestion and fillers or other components. Examination of relative Ca to S concentrations found a ratio of 1.25 for gypsum and 1.11 for the sample. There may be S-containing fillers in the drywall, but the bulk of the Ca and S likely comes from gypsum. Other ash samples collected were considered to be mixtures of many materials, not mono-material samples. Although there is generally reasonable agreement between bulk and post combustion mass percentages for the examples cited, there are still many unknowns as to how combustion impacts the final metal content in ash generally. More work across a diverse range of samples is necessary to determine if these trends in metal behavior are significant at temperatures seen during combustion of a structure.

Trace Metals Present in Water Leach

The solubility of trace metals in water provides insight into the potential for environmental metal mobilization. Rainfall or snowmelt can transport metals to soils, groundwaters, surface waters, and agricultural areas, creating a vector of exposure to humans and animals[51–53,91]. Absolute metal concentration (g metal/g ash or soil) informs on the total mass of metals that can potentially be mobilized at a given site. This is relevant to the total environmental input, with impacts ranging from acute toxicity to increased trace metal cycling and environmental recalcitrance. Higher variability in water labile metals was observed in ash samples compared to soils (Figure 1b). Water leachable Cu concentrations in ash samples ranged from 0.009-2.95 mg/kg, with an average of 0.44 mg/kg. Soil samples showed less variation (0.016-0.133 mg/kg), with an average of 0.064 mg/kg. There was no significant difference in median Cu concentrations between ash and soil ($p=0.92$). Ash samples leached significantly more Cr compared to the soil samples ($p=4.3E-4$). Ash ranged from 0.17-3.93 mg/kg Cr with an average of 1.13 mg/kg. The soil samples were more uniform in their leaching behavior and released between 0.029-0.039 mg/kg Cr with an average of 0.030 mg/kg. Ash leached significantly more Ni than the soils and had a higher median concentration ($p=0.0041$). Ni concentration in ash samples was the most variable of all water leachable metals reported and ranged from 0.013-0.795 mg/kg with an average of 0.31 mg/kg. In contrast, the soil sample leached between 0.009-0.035 mg/kg and with an average of 0.026 mg/kg. While the acid-extractable Ni concentrations were similar between ash and soil, the greater concentration of water-soluble Ni in ash as compared to soil suggests that the ash samples have higher concentration of mobilizable Ni. There is evidence that the conditions during combustion can transform Ni species to $NiSO_4$ in coal and soil, altering its solubility, bioavailability, and subsequent environmental mobility[58]. These changes in speciation can also increase the toxicity of Ni, creating concern for aquatic species. Ash

was observed by SEM (Figure S2a-b) to be porous, which may contribute to the leaching of metals due to high surface area for sorption. Water leachable Pb showed no significant differences between the soil and ash samples ($p=0.099$) and had higher variability within ash samples than in soils. Pb in the soil samples ranged from 0.006-0.11 mg/kg with an average of 0.009 mg/kg while ash samples ranged from LOQ-0.046 mg/kg with an average of 0.009 mg/kg.

Speciation of metals is a determining factor in their solubility[61]. Combustion can alter the speciation of metals via oxidation[57–60], altering metal mobility, toxicity, and bioavailability. Percent leached (g metal leached /g acid extractable metal) was calculated (Figure 3a) to examine relative leachability of metals. Although the total concentration of Cu liberated in water leach was similar between the ash and soil samples (Figure 1a), ash samples leached an average of 0.10% Cu while soil samples leached 0.41% Cu. On average, Pb in the ash samples leached at a similar percentage to that of the soil samples, 0.16% and 0.13%, despite significantly higher acid extractable Pb concentrations present in ash. The ash samples had a lower proportion of weakly soluble sorbed Pb and Cu than soil samples, despite containing more total Cu and Pb. The lower leachability of Cu and Pb post combustion may be due to the presence of biochar derived from wood in the ash, which has been shown to limit Cu and Pb mobility[95,96]. Ash samples leached a higher percentage of Ni and Cr than soil samples. Ash leached an average of 3.62% and 1.13% for Ni and Cr, respectively while soils leached 0.31% of Ni and 0.56% of Cr. Acid extractable Ni and Cr content was not significantly different between the ash and soil samples, but ash samples contained a higher proportion of labile metals. The elevated Cr leachability in ash compared to soils is likely due to combustion mediated transformation of Cr. Cr in soils exists as Cr (III), an insoluble cation and Cr (VI), a highly toxic and mobile form[57,60]. Studies have shown that combustion can oxidize Cr (III) to Cr (VI), in soils and even in CCA treated woods[57,60,67,97,98]. Transformation of Cr (III) to Cr (VI) is highly favorable at 400 °C, a temperature that burning structures easily reach[57,60]. Wildfires can increase metal mobility[43,99], and elevated concentrations of water leachable Ni have been reported in runoff from burned areas[100], likely due to the increase in bioavailable Ni forms post combustion[58].

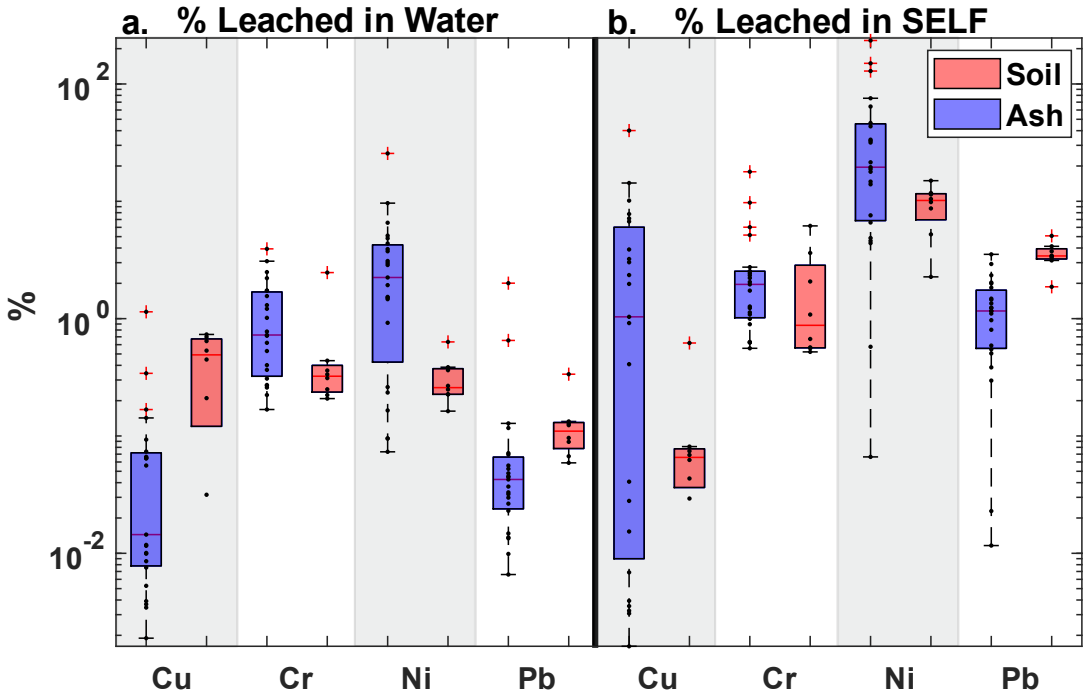

Figure 3. *Box and whisker plot showing percent of metals leached in a) water leach and b) SELF leach. Percent is based on acid leach as a total metal concentration. Soil samples are shown in red, ash samples are shown in blue. Exact percent for each sample are shown as black dots, outliers are shown as red "+". Red line shows median, box edges show 25-75th percentile, whiskers cover 99.3 percent of data.*

Bioaccessibility of Trace Metals in Simulated Epithelial Lung Fluid (SELF) Leach

The concentrations of metals extracted by SELF leach across sample locations at S1 are shown as bubble plots (Figure 4a-d), and site composites S2-4 are shown in Figure S3. The respiratory leachable concentration in ash ranged from BDL-208 mg/kg for Cu, 0.1-1.9 mg/kg Cr, BDL-7.4 mg/kg Ni, and BDL-1.7 mg/kg Pb in ash samples. For soil samples, the respiratory leachable concentration ranged from BDL-1.0 mg/kg Cu, 0.1-0.3 mg/kg Cr, BDL-1.4 mg/kg Ni, and 0.1-0.5 mg/kg Pb. These reported values are likely conservative estimate of SELF soluble metal concentrations. Studies have found that the <10 µm ash fraction typically contains a higher concentration of metal than the larger material used in this study[74,101], and is of a size that is more likely to be respired. However, due to laboratory constraints and in order to draw comparison with the acid and water leach, the <2mm fraction was used in the SELF leach.

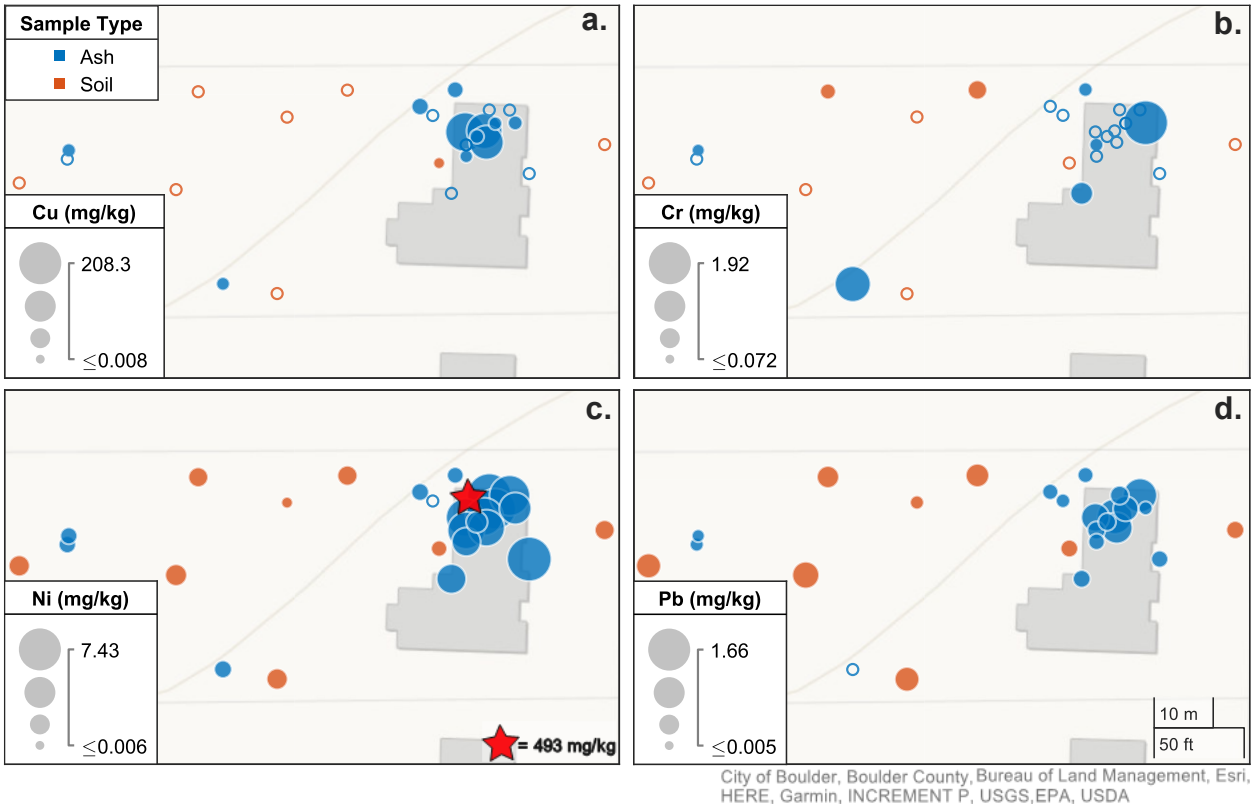

Figure 4. Bubble plots show spatial distribution of metal concentration at samples locations at Site S-1. Orange circles represent concentrations in soil samples, and blue circles represent ash samples. Hallow circles are used to designate samples below the limit of quantification that are reported as the LOQ (See SI for calculations). Ni outlier plotted as a star.

Ash samples were significantly higher in Cu compared to soil samples (p=0.013). Approximately 38% of all samples extracted with SELF were below the instrumental detection limit or the LOQ. Only one soil sample was above the LOQ. Soil and ash samples do not show significant differences in Cr concentration (p=0.35) and 52% of samples were below the Cr instrumental detection limit. Samples that had the highest measurable concentrations of Cr included a sample from the garage (1.92 mg/kg), where paint and other tools were stored, and the burned tire material used in a playground (1.22 mg/kg). Ni content was significantly higher in the ash samples as compared to soil samples (p=0.036), with only 3% of samples below the instrumental detection limit. There was also no significant difference in concentration between soil and ash samples for Pb (p=0.33), with approximately 10% of samples below instrumental detection limit. Inhalation bioaccessibility was also calculated as percent of acid extractable metal content (Figure 3b). The percentage of metals extracted in SELF were highly variable, both between and within ash and soil samples. The Cu bioaccessibility in ash ranged from 0-40% with an average of 4.48%. In soil samples, the percent of bioaccessible Cu ranged from 0-0.62% with an average of 0.12%. There were no significant differences between the soil and ash samples with respect to the percent of Cu leached in SELF. High variability was observed in the percent of Cu leached in the ash samples, especially when compared to the soils. In ash, the percentage of Cr ranged from 0.56-17.86% with an average of 2.97%. Cr ranged from 0.52-6.17% with an average of 1.91% in soils, making Cr moderately more bioaccessible in ash samples. The percentage of bioaccessible Ni ranged from 0.07-234% with an average of 42.46% in

ash. There were 3 ash samples with over 100% bioaccessibility in the SELF leach. These outliers were at the lower end of the concentration (between 3.1-5.8 mg/kg of acid leachable Ni), and so the high percentage is attributed to increased analytical error at lower concentrations. In soils, the percent of leachable Ni ranged from 2.27-14.99% with an average of 9.34%. There was no significant enrichment of acid soluble Ni in the ash over soil, however, increased overall bioaccessibility was observed in the ash samples compared to the soils, suggesting that Ni may be in a form that is more soluble in the SELF matrix. Pb bioaccessibility in ash ranged 0.1-3.53% with an average of 1.26%. In soils, the percentage of leachable Pb ranged from 1.87-5.08% with an average to 3.52%. Pb bioaccessibility was significantly higher in soil samples than in the ash, suggesting that there may be a difference in the speciation of Pb between the sample types. The variability in the percent leachable was high for Cu, Ni, and Pb in the SELF. High variability within bioaccessibility suggests that total metal content as quantified in an acid leach is not a suitable predictor for the bioaccessibility of that metal in ash. More work to determine the speciation of metals, and what role this may play in prediction of bioaccessibility is needed.

The chemical composition of SELF impacts the solubility of metals. The organic and acid constituents in SELF can chelate with some metals, causing increased solubility[82]. Glycoproteins such as albumin and mucin bind with metals and can be controlling factors in bioaccessibility. However, mucin has been reported to form precipitates with Pb^{2+} at neutral pH (SELF pH 7.4). This may reduce Pb solubility[75]. Additionally, the speciation of the metals will continue to dictate their interactions with the molecules in the SELF and subsequently influence solubility. The elevated concentrations of Ni and Cu leachable in SELF have implications for human health, especially for individuals who are involved in site clean-up, or are exposed to ash spread by post-fire wind events. Ni and Cu are important for biologic function at low concentrations, but overexposure has been linked to adverse health effects. Excess Ni causes toxicity and respiratory disorders and is dependent on solubility in lung[83,101]. The primary routes of Ni exposure in humans are inhalation, ingestion, and dermal contact[102] warranting the further investigation into the bioaccessibility of Ni in WUI ash. Cu exposure has been linked to neurodegenerative effects and oxidative stress, although excretory processes protect against acute Cu toxicity for most humans and animals[103]. While the authors are unaware of studies that have explored the bioaccessibility of trace metals in ash derived for structure fires, studies have explored trace metals in volcanic and coal fly ash[82,83,104]. However, results varied widely between materials, and it is unlikely that these results can be compared with structural ash, as ash composition and mineralogy dictate bioaccessibilty[74,82].

Correlations

Correlation analysis was used to identify relationships between metals that may be influenced by geogenic or anthropogenic material composition, as well as provide insight into which metals may drive ash toxicity. We found a strong correlation between the acid leachable Pb and Cu (r=0.88) in the ash samples (Figure S4a). Pb and Cu are commonly used together in electronics and wiring, which may contribute to the correlation. We also found moderately strong to strong correlations between acid leachable Cr-Al (r=0.74) and Cr-Fe (r=0.86) in the ash (SI 3a). Cr is added to iron in order to create stronger alloys, including stainless steel, which could account for its association in the ash. Cr co-occurs naturally with iron as chromite ($FeCr_2O_4$); however, Colorado is not known to be a significant site of this mineral[105]. Without further investigation into the speciation or form of Cr, it is not possible to determine if the correlation is due to natural or anthropogenic associations. No correlations were found for the ash samples in the water leach or in the SELF leach (Figure S5a, 6a), which we attributed to the heterogeneity of the ash. The ash samples were derived from combustion of a wide range of materials in the structures, leading to high variability in metal concentrations. There is spatial variation in metal concentration when structures burn and supports that assumption that there is no common metal concentration in WUI ash.

In contrast to the ash, we found many strong correlations between metals in the soil samples. We found strong correlations between acid leachable Cr-Ni (r=0.82), Cr-Al (r=0.76), Ni-Pb (r= 0.82), Ni-Fe (r=0.91), Pb-Al (r=0.87), Pb-Fe (r=0.85), and Al-Fe (r=0.87) (SI 3b). Correlations for soils in Colorado were also calculated using data from a 2006 USGS study [84],which found a strong correlation between Cr-Ni (r=0.86). However no strong correlations were found between the other metals reported. Although correlations between metals in soils at this site differ from the USGS values, it is likely that high correlations exist due to the small area sampled. Iron and aluminum are major elements in the Earth's crust and co-occur in soils and minerals. The associations of Pb and Ni with Fe suggest that they may be bound to iron oxides, which has been reported at other locations in Colorado[106]. Water leachable metal correlations included Cd-Cu (r=0.86), Cu-Pb (r=0.82), and Cd-Pb (r=0.87) (Figure S5b). It should be noted that the water leachable concentrations of these metals were generally low, and so may be subject to increased analytical noise associated with concentrations near detection limits. The only strong correlation for the soil samples in the SELF leach was Ni-Pb (r=0.89) (Figure S6b). This is a similar correlation as was seen for these metals in the acid leach and may indicate that minerals containing these metals exhibit similar solubilities. Across all soil and ash samples, there was a strong correlation between the amount of water leachable and SELF leachable Ni (r=0.86) (SI 8). There was a moderately strong correlation (r=0.69) between the water and SELF leachable Cr. This suggests that the water leachable Ni and Cr concentrations may provide insight into the bioaccessibility of these metals in the human lung. There is also a correlation between the acid and SELF leachable Pb (r=0.85) and a weak (r=0.58) correlation between acid and SELF leachable Cu.

Environmental Significance. We characterized the environmental lability and respiratory bioaccessibility of metals in ash from structure fires in the WUI and found that ash is a source of trace metals to the environment, and to humans. The quantities of ash generated during large scale WUI fires, such as the Marshall Fire, have the potential to negatively impact the surrounding environment, agriculture, communities, first responders, and residents. Metals can be mobilized via rainfall or snowmelt, thereby influencing aquatic toxicity, physiochemical properties of surface water, and elevating soil metal concentration[41,43,107]. SELF has been used to determine inhalation bioaccessibility of metals in materials including volcanic ash, fly ash, soils, and road dusts[74,83,101,104,108], however it has not previously been used for WUI ash. Despite elevated metal content in WUI ash and increased solubility of certain metals compared to soils, the role that combustion plays on bulk scale metals is still poorly understood. Additionally, higher solubility (% leachable) in ash compared to soils may be influenced by combustion driven changes in metal form[57–60,97]. Combustion has been shown to impact metals by altering speciation through redox mechanisms (Cr)[57,60,97] as well as vaporization and condensation (Cd, Pb)[44,58,61] in soils and coal. Further work is needed to determine if this mechanism is active in a structure fire scenario, where temperatures are typically recorded between 400-500 °C[88], and how these mechanisms impact bulk scale metals that are present in structures. As the United States continues to face more severe wildfire seasons, there is a greater need to understand wildfire impact on metal bioaccessibility and environmental toxicity, especially in a WUI setting. This research provides a framework for assessing the solubility of metals in ash generated from WUI fires in environmentally and biologically relevant matrices.

Supporting Information: Additional experimental details including sample location map, equations, SEM images, and correlation matrix plots.

Acknowledgements

We would like to acknowledge the homeowners who provided us access to their properties for sampling purposes. We would also like to thank Dr. John Spear, Aaron Goodman, and Zhaoxun Yang. Funding provided by National Science Foundation CBET 2217526

References

(1) Higuera, P. E.; Abatzoglou, J. T.; Littell, J. S.; Morgan, P. The Changing Strength and Nature of Fire-Climate Relationships in the Northern Rocky Mountains, U.S.A., 1902-2008. *PLoS One* **2015**, *10* (6), 1–21. https://doi.org/10.1371/journal.pone.0127563.

(2) Schoennagel, T.; Balch, J. K.; Brenkert-Smith, H.; Dennison, P. E.; Harvey, B. J.; Krawchuk, M. A.; Mietkiewicz, N.; Morgan, P.; Moritz, M. A.; Rasker, R.; Turner, M. G.; Whitlock, C. Adapt to More Wildfire in Western North American Forests as Climate Changes. *Proceedings of the National Academy of Sciences* **2017**, *114* (18), 4582–4590. https://doi.org/10.1073/pnas.1617464114.

(3) Keeley, J. E.; Syphard, A. D. Climate Change and Future Fire Regimes: Examples from California. *Geosciences (Basel)* **2016**, *6* (3), 1–14. https://doi.org/10.3390/geosciences6030037.

(4) Abatzoglou, J. T.; Williams, A. P.; Barbero, R. Global Emergence of Anthropogenic Climate Change in Fire Weather Indices. *Geophys Res Lett* **2019**, *46* (1), 326–336. https://doi.org/10.1029/2018GL080959.

(5) Westerling, A. L.; Hidalgo, H. G.; Swetman, T. W. Warming and Earlier Spring Increase Western U.S. Forest Wildfire Activity. *Science (1979)* **2006**, *313*, 940–944.

(6) Dupuy, J. luc; Fargeon, H.; Martin-StPaul, N.; Pimont, F.; Ruffault, J.; Guijarro, M.; Hernando, C.; Madrigal, J.; Fernandes, P. Climate Change Impact on Future Wildfire Danger and Activity in Southern Europe: A Review. *Ann For Sci* **2020**, *77* (2). https://doi.org/10.1007/s13595-020-00933-5.

(7) Mansoor, S.; Farooq, I.; Kachroo, M. M.; Mahmoud, A. E. D.; Fawzy, M.; Popescu, S. M.; Alyemeni, M. N.; Sonne, C.; Rinklebe, J.; Ahmad, P. Elevation in Wildfire Frequencies with Respect to the Climate Change. *J Environ Manage* **2022**, *301*, 113769. https://doi.org/10.1016/j.jenvman.2021.113769.

(8) Abatzoglou, J. T.; Williams, A. P. Impact of Anthropogenic Climate Change on Wildfire across Western US Forests. *Proc Natl Acad Sci U S A* **2016**, *113* (42), 11770–11775. https://doi.org/10.1073/pnas.1607171113.

(9) Marlon, J. R.; Bartlein, P. J.; Gavin, D. G.; Long, C. J.; Anderson, R. S.; Briles, C. E.; Brown, K. J.; Colombaroli, D.; Hallett, D. J.; Power, M. J.; Scharf, E. A.; Walsh, M. K. Long-Term Perspective on Wildfires in the Western USA. *Proc Natl Acad Sci U S A* **2012**, *109* (9), 535–543. https://doi.org/10.1073/pnas.1112839109.

(10) Clarke, H.; Nolan, R. H.; Dios, V. R. De; Bradstock, R.; Griebel, A.; Khanal, S.; Boer, M. M. Forest Fire Threatens Global Carbon Sinks and Population Centres under Rising Atmospheric Water Demand. *Nat Commun* **2022**, *13*, 1–10. https://doi.org/10.1038/s41467-022-34966-3.

(11) Iglesias, V.; Balch, J. K.; Travis, W. R. U.S. Fires Became Larger, More Frequent, and More Widespread in the 2000s. *Sci Adv* **2022**, *8*.

(12) Hoover, K.; Hanson, L. A. Wildfire Statistics. *Congressional Research Service* **2021**, 2.

(13) *Statistics | National Interagency Fire Center*. https://www.nifc.gov/fire-information/statistics.

(14) Radeloff, V. C.; Hammer, R. B.; Stewart, S. I.; Fried, J. S.; Holcomb, S. S.; McKeefry, J. F. THE WILDLAND – URBAN INTERFACE IN THE UNITED STATES. *Ecological Applications* **2005**, *15* (3), 799–805.

(15) Hanberry, B. B. Reclassifying the Wildland – Urban Interface Using Fire Occurrences for the United States. *Land (Basel)* **2020**, *9* (7).

(16) Haight, R. G.; Cleland, D. T.; Hammer, R. B.; Radeloff, V. C.; Rupp, T. S. Assessing Fire Risk in the Wildland-Urban Interface. *J For* **2004**, *102* (7), 41–47.

(17) Kramer, H. A.; Mockrin, M. H.; Alexandre, P. M.; Radeloff, V. C. High Wildfire Damage in Interface Communities in California. *Int J Wildland Fire* **2019**, *28* (9), 641–650. https://doi.org/10.1071/WF18108.

(18) Radeloff, V. C.; Helmers, D. P.; Anu Kramer, H.; Mockrin, M. H.; Alexandre, P. M.; Bar-Massada, A.; Butsic, V.; Hawbaker, T. J.; Martinuzzi, S.; Syphard, A. D.; Stewart, S. I. Rapid Growth of the US Wildland-Urban Interface Raises Wildfire Risk. *Proc Natl Acad Sci U S A* **2018**, *115* (13), 3314–3319. https://doi.org/10.1073/pnas.1718850115.

(19) Burke, M.; Driscoll, A.; Heft-Neal, S.; Xue, J.; Burney, J.; Wara, M. The Changing Risk and Burden of Wildfire in the United States. *Proc Natl Acad Sci U S A* **2021**, *118* (2), 1–6. https://doi.org/10.1073/PNAS.2011048118.

(20) Clark, M. B.; Nkonya, E.; Galford, G. L. Flocking to Fire : How Climate and Natural Hazards Shape Human Migration across the United States. *Frontiers in Human Dynamics* **2022**, *4*.

(21) Liu, J. C.; Pereira, G.; Uhl, S. A.; Bravo, M. A.; Bell, M. L. A Systematic Review of the Physical Health Impacts from Non-Occupational Exposure to Wildfire Smoke. *Environ Res* **2015**, *136*, 120–132. https://doi.org/10.1016/j.envres.2014.10.015.

(22) Abdo, M.; Ward, I.; O'dell, K.; Ford, B.; Pierce, J. R.; Fischer, E. V.; Crooks, J. L. Impact of Wildfire Smoke on Adverse Pregnancy Outcomes in Colorado, 2007–2015. *Int J Environ Res Public Health* **2019**, *16* (19). https://doi.org/10.3390/ijerph16193720.

(23) Caumo, S.; Lázaro, W. L.; Sobreira Oliveira, E.; Beringui, K.; Gioda, A.; Massone, C. G.; Carreira, R.; de Freitas, D. S.; Ignacio, A. R. A.; Hacon, S. Human Risk Assessment of Ash Soil after 2020 Wildfires in Pantanal Biome (Brazil). *Air Qual Atmos Health* **2022**. https://doi.org/10.1007/s11869-022-01248-2.

(24) Adetona, O.; Reinhardt, T. E.; Domitrovich, J.; Broyles, G.; Adetona, A. M.; Kleinman, M. T.; Ottmar, R. D.; Naeher, L. P. Review of the Health Effects of Wildland Fire Smoke on Wildland Firefighters and the Public. *Inhal Toxicol* **2016**, *28* (3), 95–139. https://doi.org/10.3109/08958378.2016.1145771.

(25) Cascio, W. E. Wildland Fire Smoke and Human Health. *Science of the Total Environment* **2018**, *624*, 586–595. https://doi.org/10.1016/j.scitotenv.2017.12.086.

(26) Reid, C. E.; Brauer, M.; Johnston, F. H.; Jerrett, M.; Balmes, J. R.; Elliott, C. T. Critical Review of Health Impacts of Wildfire Smoke Exposure. *Environ Health Perspect* **2016**, *124* (9), 1334–1343. https://doi.org/10.1289/ehp.1409277.

(27) Stowell, J. D.; Yang, C. E.; Fu, J. S.; Scovronick, N. C.; Strickland, M. J.; Liu, Y. Asthma Exacerbation Due to Climate Change-Induced Wildfire Smoke in the Western US. *Environmental Research Letters* **2022**, *17* (1). https://doi.org/10.1088/1748-9326/ac4138.

(28) Delfino, R. J.; Brummel, S.; Wu, J.; Stern, H.; Ostro, B.; Lipsett, M.; Winer, A.; Street, D. H.; Zhang, L.; Tjoa, T.; Gillen, D. L. The Relationship of Respiratory and Cardiovascular Hospital Admissions to the Southern California Wildfires of 2003. *Occup Environ Med* **2009**, *66* (3), 189–197. https://doi.org/10.1136/oem.2008.041376.

(29) Nakayama Wong, L. S.; Aung, H. H.; Lamé, M. W.; Wegesser, T. C.; Wilson, D. W. Fine Particulate Matter from Urban Ambient and Wildfire Sources from California's San Joaquin Valley Initiate Differential Inflammatory, Oxidative Stress, and Xenobiotic Responses in Human Bronchial Epithelial Cells. *Toxicology in Vitro* **2011**, *25* (8), 1895–1905. https://doi.org/10.1016/j.tiv.2011.06.001.

(30) Liu, Y.; Austin, E.; Xiang, J.; Gould, T.; Larson, T.; Seto, E. Health Impact Assessment of the 2020 Washington State Wildfire Smoke Episode: Excess Health Burden Attributable to Increased PM2.5 Exposures and Potential Exposure Reductions. *Geohealth* **2021**, *5* (5), 1–11. https://doi.org/10.1029/2020GH000359.

(31) Morgan, G.; Sheppeard, V.; Khalaj, B.; Ayyar, A.; Lincoln, D.; Jalaludin, B.; Beard, J.; Corbett, S.; Lumley, T. Effects of Bushfire Smoke on Daily Mortality and Hospital Admissions in Sydney, Australia. *Epidemiology* **2010**, *21* (1), 47–55. https://doi.org/10.1097/EDE.0b013e3181c15d5a.

(32) Alman, B. L.; Pfister, G.; Hao, H.; Stowell, J.; Hu, X.; Liu, Y.; Strickland, M. J. The Association of Wildfire Smoke with Respiratory and Cardiovascular Emergency Department Visits in Colorado in 2012: A Case Crossover Study. *Envrionmental Health* **2016**, *15* (1), 1–9. https://doi.org/10.1186/s12940-016-0146-8.

(33) Holstius, D. M.; Reid, C. E.; Jesdale, B. M.; Morello-Frosch, R. Birth Weight Following Pregnancy during the 2003 Southern California Wildfires. *Environ Health Perspect* **2012**, *120* (9), 1340–1345. https://doi.org/10.1289/ehp.1104515.

(34) Lee, K.; Oh, S.; Jeong, K. S.; Ahn, Y.; Chang, S. J.; Hong, S. H.; Kang, D. R.; Kim, S.; Koh, S. Impact of Wildfire Smoke Exposure on Health in Korea. *Yonsei Med J* **2022**, *63* (8), 774–782.

(35) Bowman, D. M. J. S.; Johnston, F. H. Wildfire Smoke, Fire Management, and Human Health. *Ecohealth* **2005**, *2* (1), 76–80. https://doi.org/10.1007/s10393-004-0149-8.

(36) Requia, W. J.; Amini, H.; Mukherjee, R.; Gold, D. R.; Schwartz, J. D. Health Impacts of Wildfire-Related Air Pollution in Brazil: A Nationwide Study of More than 2 Million Hospital Admissions between 2008 and 2018. *Nat Commun* **2021**, *12* (1), 1–10. https://doi.org/10.1038/s41467-021-26822-7.

(37) Korsiak, J.; Pinault, L.; Christidis, T.; Burnett, R. T.; Abrahamowicz, M.; Weichenthal, S. Long-Term Exposure to Wildfires and Cancer Incidence in Canada : A Population-Based Observational Cohort Study. *Lancet Planet Health* **2022**, *6* (5), e400–e409. https://doi.org/10.1016/S2542-5196(22)00067-5.

(38) Bloom, T. D. S.; Flower, A.; Medler, M.; DeChaine, E. G. The Compounding Consequences of Wildfire and Climate Change for a High-Elevation Wildflower (Saxifraga Austromontana). *J Biogeogr* **2018**, *45* (12), 2755–2765. https://doi.org/10.1111/jbi.13441.

(39) Seidl, R.; Spies, T. A.; Peterson, D. L.; Stephens, S. L.; Jeffrey, A. Searching for Resilience : Addressing the Impacts of Changing Disturbance Regimes on Forest Ecosystem Services. *Journal of Applied Ecology* **2016**, *53*, 120–129. https://doi.org/10.1111/1365-2664.12511.

(40) Blakey, R. V; Sikich, J. A.; Blumstein, D. T.; Riley, S. P. D.; Blakey, R. V; Sikich, J. A.; Blumstein, D. T.; Riley, S. P. D. *Report Mountain Lions Avoid Burned Areas and Increase Risky Behavior after Wildfire in a Fragmented Urban Landscape Ll Mountain Lions Avoid Burned Areas and Increase Risky Behavior after Wildfire in a Fragmented Urban Landscape*; The Authors, 2022; Vol. 32. https://doi.org/10.1016/j.cub.2022.08.082.

(41) Gomez Isaza, D. F.; Cramp, R. L.; Franklin, C. E. Fire and Rain: A Systematic Review of the Impacts of Wildfire and Associated Runoff on Aquatic Fauna. *Glob Chang Biol* **2022**, *28* (8), 2578–2595. https://doi.org/10.1111/gcb.16088.

(42) Palmer, J. The Devastating Mudslides That Follow Forest Fires. *Nature*. 2022, pp 184–186. https://doi.org/10.1038/d41586-022-00028-3.

(43) Abraham, J.; Dowling, K.; Florentine, S. The Unquantified Risk of Post-Fire Metal Concentration in Soil: A Review. *Water Air Soil Pollut* **2017**, *228* (5). https://doi.org/10.1007/s11270-017-3338-0.

(44) Senior, C. L.; Bool, L. E.; Srinivasachar, S.; Pease, B. R.; Porle, K. Pilot Scale Study of Trace Element Vaporization and Condensation during Combustion of a Pulverized Sub-Bituminous Coal. *Fuel processing technology* **2000**, *63* (2), 149–165. https://doi.org/10.1016/S0378-3820(99)00094-6.

(45) Susaya, J.; Kim, K. H.; Ahn, J. W.; Jung, M. C.; Kang, C. H. BBQ Charcoal Combustion as an Important Source of Trace Metal Exposure to Humans. *J Hazard Mater* **2010**, *176* (1–3), 932–937. https://doi.org/10.1016/j.jhazmat.2009.11.129.

(46) Kelly, R. L.; Bian, X.; Feakins, S. J.; Fornace, K. L.; Gunderson, T.; Hawco, N. J.; Liang, H.; Niggemann, J.; Paulson, S. E.; Pinedo-Gonzalez, P.; West, A. J.; Yang, S. C.; John, S. G. Delivery of Metals and Dissolved Black Carbon to the Southern California Coastal Ocean via Aerosols and Floodwaters Following the 2017 Thomas Fire. *J Geophys Res Biogeosci* **2021**, *126* (3), 1–25. https://doi.org/10.1029/2020JG006117.

(47) Costa, M. R.; Calvão, A. R.; Aranha, J. Linking Wildfire Effects on Soil and Water Chemistry of the Marão River Watershed, Portugal, and Biomass Changes Detected from Landsat Imagery. *Applied Geochemistry* **2014**, *44*, 93–102. https://doi.org/10.1016/j.apgeochem.2013.09.009.

(48) Rahman, A.; El Hayek, E.; Blake, J. M.; Bixby, R. J.; Ali, A. M.; Spilde, M.; Otieno, A. A.; Miltenberger, K.; Ridgeway, C.; Artyushkova, K.; Atudorei, V.; Cerrato, J. M. Metal Reactivity in Laboratory Burned Wood from a Watershed Affected by Wildfires. *Environ Sci Technol* **2018**, *52* (15), 8115–8123. https://doi.org/10.1021/acs.est.8b00530.

(49) Burke, M. P.; Hogue, T. S.; Kinoshita, A. M.; Barco, J.; Wessel, C.; Stein, E. D. Pre- and Post-Fire Pollutant Loads in an Urban Fringe Watershed in Southern California. *Environ Monit Assess* **2013**, *185* (12), 10131–10145. https://doi.org/10.1007/s10661-013-3318-9.

(50) Emmerton, C. A.; Cooke, C. A.; Hustins, S.; Silins, U.; Emelko, M. B.; Lewis, T.; Kruk, M. K.; Taube, N.; Zhu, D.; Jackson, B.; Stone, M.; Kerr, J. G.; Orwin, J. F. Severe Western Canadian Wildfire Affects Water Quality Even at Large Basin Scales. *Water Res* **2020**, *183*, 116071. https://doi.org/10.1016/j.watres.2020.116071.

(51) Pereira, P.; Úbeda, X. Spatial Distribution of Heavy Metals Released from Ashes after a Wildfire. *Journal of Environmental Engineering and Landscape Management* **2010**, *18* (1), 13–22. https://doi.org/10.3846/jeelm.2010.02.

(52) Pradhan, A.; Carvalho, F.; Abrantes, N.; Campos, I.; Keizer, J. J.; Cássio, F.; Pascoal, C. Biochemical and Functional Responses of Stream Invertebrate Shredders to Post-Wildfire Contamination. *Environmental Pollution* **2020**, *267*. https://doi.org/10.1016/j.envpol.2020.115433.

(53) Paul, M. J.; LeDuc, S. D.; Lassiter, M. G.; Moorhead, L. C.; Noyes, P. D.; Leibowitz, S. G. Wildfire Induces Changes in Receiving Waters: A Review With Considerations for Water Quality Management. *Water Resour Res* **2022**, *58* (9). https://doi.org/10.1029/2021WR030699.

(54) East, A. E.; Logan, J. B.; Dartnell, P.; Lieber-kotz, O.; Cavagnaro, D. B.; McCoy, S. W.; Lindsay, D. N. Watershed Sediment Yield Following the 2018 Carr Fire , Whiskeytown National Recreation Area , Northern California. *Earth and Space Science* **2021**, *8*. https://doi.org/10.1029/2021EA001828.

(55) Baieta, R.; Vieira, A. M. D.; Vaňková, M.; Mihaljevič, M. Effects of Forest Fires on Soil Lead Elemental Contents and Isotopic Ratios. *Geoderma* **2022**, *414* (February). https://doi.org/10.1016/j.geoderma.2022.115760.

(56) Campos, I.; Abrantes, N.; Keizer, J. J.; Vale, C.; Pereira, P. Major and Trace Elements in Soils and Ashes of Eucalypt and Pine Forest Plantations in Portugal Following a Wildfire. *Science of the Total Environment* **2016**, *572*, 1363–1376. https://doi.org/10.1016/j.scitotenv.2016.01.190.

(57) Burton, E. D.; Choppala, G.; Vithana, C. L.; Karimian, N.; Hockmann, K.; Johnston, S. G. Chromium(VI) Formation via Heating of Cr(III)-Fe(III)-(Oxy)Hydroxides: A Pathway for Fire-Induced Soil Pollution. *Chemosphere* **2019**, *222*, 440–444. https://doi.org/10.1016/j.chemosphere.2019.01.172.

(58) Shah, P.; Vladimir, S.; Nelson, P. F. X-Ray Absorption near Edge Structure Spectrometry Study of Nickel and Lead Speciation in Coals and Coal Combustion Products. *Energy and Fuels* **2009**, *23* (3), 1518–1525. https://doi.org/10.1021/ef800824d.

(59) Zha, J.; Huang, Y.; Zhu, Z.; Yu, M.; Clough, P. T.; Yan, Y.; Dong, L.; Cheng, H. Dynamic Transformations of Metals in the Burning Solid Matter during Combustion of Heavy Metal-Contaminated Biomass. *ACS Sustain Chem Eng* **2021**, *9* (20), 7063–7073. https://doi.org/10.1021/acssuschemeng.1c01048.

(60) Burton, E. D.; Choppala, G.; Karimian, N.; Johnston, S. G. A New Pathway for Hexavalent Chromium Formation in Soil: Fire-Induced Alteration of Iron Oxides. *Environmental Pollution* **2019**, *247*, 618–625. https://doi.org/10.1016/j.envpol.2019.01.094.

(61) Linak, W. P.; Wendt, J. O. L. Trace Metal Transformation Mechanisms during Coal Combustion. *Fuel Processing Technology* **1994**, *39* (1–3), 173–198. https://doi.org/10.1016/0378-3820(94)90179-1.

(62) Etiégni, L.; Campbell, A. G. Physical and Chemical Characteristics of Wood Ash. *Bioresour Technol* **1991**, *37* (2), 173–178. https://doi.org/10.1016/0960-8524(91)90207-Z.

(63) Abraham, J.; Dowling, K.; Florentine, S. Risk of Post-Fire Metal Mobilization into Surface Water Resources: A Review. *Science of the Total Environment* **2017**, *599–600*, 1740–1755. https://doi.org/10.1016/j.scitotenv.2017.05.096.

(64) Olafisoye, O. B.; Adefioye, T.; Osibote, O. A. Heavy Metals Contamination of Water, Soil, and Plants around an Electronic Waste Dumpsite. *Pol J Environ Stud* **2013**, *22* (5), 1431–1439.

(65) Karel Houessionon, M. G.; Ouendo, E. M. D.; Bouland, C.; Takyi, S. A.; Kedote, N. M.; Fayomi, B.; Fobil, J. N.; Basu, N. Environmental Heavy Metal Contamination from Electronic Waste (E-Waste) Recycling Activities Worldwide: A Systematic Review from 2005 to 2017. *Int J Environ Res Public Health* **2021**, *18* (7). https://doi.org/10.3390/ijerph18073517.

(66) Wu, W.; Wu, P.; Yang, F.; Sun, D. ling; Zhang, D. X.; Zhou, Y. K. Assessment of Heavy Metal Pollution and Human Health Risks in Urban Soils around an Electronics Manufacturing Facility. *Science of the Total Environment* **2018**, *630*, 53–61. https://doi.org/10.1016/j.scitotenv.2018.02.183.

(67) Alam, M.; Alshehri, T.; Wang, J.; Singerling, S. A.; Alpers, C. N.; Baalousha, M. Identification and Quantification of Cr, Cu, and As Incidental Nanomaterials Derived from CCA-Treated Wood in Wildland-Urban Interface Fire Ashes. *J Hazard Mater* **2023**, *445* (November 2022), 130608. https://doi.org/10.1016/j.jhazmat.2022.130608.

(68) Alshehri, T.; Wang, J.; Singerling, S. A.; Gigault, J.; Webster, J. P.; Matiasek, S. J.; Alpers, C. N.; Baalousha, M. Wildland-Urban Interface Fire Ashes as a Major Source of Incidental Nanomaterials. *J Hazard Mater* **2022**, *443*, 130311. https://doi.org/10.1016/j.jhazmat.2022.130311.

(69) Pedersen, A. J.; Ottosen, L. M. Elemental Analysis of Ash Residue from Combustion of CCA Treated Wood Waste before and after Electrodialytic Extraction. *Chemosphere* **2006**, *65* (1), 110–116. https://doi.org/10.1016/j.chemosphere.2006.02.021.

(70) Gagas, D. Characterization of Contaminants on Firefighter's Protective Equipment: A Firefighter's Potential Exposure to Heavy Metals during a Structure Fire, 2015. https://manchester.idm.oclc.org/login?url=https://search.proquest.com/docview/1679469562?accountid=12253%0Ahttp://man-fe.hosted.exlibrisgroup.com/openurl/44MAN/44MAN_services_page?genre=dissertations+%26+theses&atitle=&author=Gagas%2C+Donald&volume=&issue.

(71) Stein, S. M.; Menakis, J.; Carr, M. A.; Comas, S. J.; Stewart, S. I.; Cleveland, H.; Bramwell, L.; Radeloff, V. C. *Wildfire, Wildlands, and People: Understanding and Preparing for Wildfire in the Wildland-Urban Interface*; 2013.

(72) Dennison, P. E.; Brewer, S. C.; Arold, J. D.; Moritz, M. A. Large Wildfire Trends in the Western United States, 1984-2011. *AGU Publications* **2014**, 2928–2933. https://doi.org/10.1002/2014GL059576.Received.

(73) Kastury, F.; Smith, E.; Juhasz, A. L. A Critical Review of Approaches and Limitations of Inhalation Bioavailability and Bioaccessibility of Metal(Loid)s from Ambient Particulate Matter or Dust. *Science of the Total Environment* **2017**, *574*, 1054–1074. https://doi.org/10.1016/j.scitotenv.2016.09.056.

(74) Drahota, P.; Raus, K.; Rychlíková, E.; Rohovec, J. Bioaccessibility of As, Cu, Pb, and Zn in Mine Waste, Urban Soil, and Road Dust in the Historical Mining Village of Kaňk, Czech Republic. *Environ Geochem Health* **2018**, *40* (4), 1495–1512. https://doi.org/10.1007/s10653-017-9999-1.

(75) Boisa, N.; Elom, N.; Dean, J. R.; Deary, M. E.; Bird, G.; Entwistle, J. A. Development and Application of an Inhalation Bioaccessibility Method (IBM) for Lead in the PM10 Size Fraction of Soil. *Environ Int* **2014**, *70*, 132–142. https://doi.org/10.1016/j.envint.2014.05.021.

(76) *Precipitation Data*. National Atmospheric Deposition Program. https://nadp.slh.wisc.edu/precipitation/ (accessed 2023-12-10).

(77) Hageman, P. L. *US Geological Survey Field Leach Test for Assessing Water Reactivity and Leaching Potential of Mine Wastes, Soils, and Other Geologic and Environmental Materials*; 2007. https://pubs.er.usgs.gov/publication/tm5D3.

(78) Creed, J.; Brockhoff, C.; Martin, T. D. Method 200.8 Determination of Trace Elements in Waters and Wastes By Inductively Coupled Plasma-Mass Spectrometry Environmental Monitoring Systems Laboratory Office of Research and Development U. *US Environmental Protection Agency* **1994**, *4*, 1–57.

(79) U.S. Environmental Protection Agency. METHOD 200.7 - Determination of Elements and Trace Elements in Water and Wastes by Inductively Coupled Plasma-Atomic Emmission Spectropemtry. *US Environmental Protection Agency* **1994**, *EPA/600/4-*, 1–58.

(80) EPA. Method 3050B Acid Digestion of Sediments, Sludges, and Soils. *EPA* **1996**, *18* (7), 723.

(81) Pelfrêne, A.; Cave, M. R.; Wragg, J.; Douay, F. In Vitro Investigations of Human Bioaccessibility from Reference Materials Using Simulated Lung Fluids. *Int J Environ Res Public Health* **2017**, *14* (2), 1–15. https://doi.org/10.3390/ijerph14020112.

(82) Tomašek, I.; Damby, D. E.; Stewart, C.; Horwell, C. J.; Plumlee, G.; Ottley, C. J.; Delmelle, P.; Morman, S.; El Yazidi, S.; Claeys, P.; Kervyn, M.; Elskens, M.; Leermakers, M. Development of a Simulated Lung Fluid Leaching Method to Assess the Release of Potentially Toxic Elements from Volcanic Ash. *Chemosphere* **2021**, *278*. https://doi.org/10.1016/j.chemosphere.2021.130303.

(83) Barone, G.; De Giudici, G.; Gimeno, D.; Lanzafame, G.; Podda, F.; Cannas, C.; Giuffrida, A.; Barchitta, M.; Agodi, A.; Mazzoleni, P. Surface Reactivity of Etna Volcanic Ash and Evaluation of

Health Risks. *Science of the Total Environment* **2021**, *761*, 143248. https://doi.org/10.1016/j.scitotenv.2020.143248.

(84) Smith, B. D. B.; Ellefsen, K. J.; Kilburn, J. E.; Survey, U. S. G. Geochemical Data for Colorado Soils : Results from the 2006 State-Scale Geochemical Survey. **2006**.

(85) Krauskopf, K. B.; Bird, D. K. *Introduction to Geochemistry*; McGraw-Hill: New York, 1967.

(86) US EPA. *Protect Your Family from Sources of Lead | US EPA*. US Environmental Protection Agency. https://www.epa.gov/lead/protect-your-family-sources-lead.

(87) US EPA. *Chromated Arsenicals (CCA) | US EPA*. https://www.epa.gov/ingredients-used-pesticide-products/chromated-arsenicals-cca.

(88) Crewe, R. J.; Stec, A. A.; Walker, R. G.; Shaw, J. E. A.; Hull, T. R.; Rhodes, J.; Garcia-Sorribes, T. Experimental Results of a Residential House Fire Test on Tenability: Temperature, Smoke, and Gas Analyses. *J Forensic Sci* **2014**, *59* (1), 139–154. https://doi.org/10.1111/1556-4029.12268.

(89) Bodí, M. B.; Martin, D. A.; Balfour, V. N.; Santín, C.; Doerr, S. H.; Pereira, P.; Cerdà, A.; Mataix-Solera, J. Wildland Fire Ash: Production, Composition and Eco-Hydro-Geomorphic Effects. *Earth Sci Rev* **2014**, *130*, 103–127. https://doi.org/10.1016/j.earscirev.2013.12.007.

(90) Stankov Jovanovic, V. P.; Ilic, M. D.; Markovic, M. S.; Mitic, V. D.; Nikolic Mandic, S. D.; Stojanovic, G. S. Wild Fire Impact on Copper, Zinc, Lead and Cadmium Distribution in Soil and Relation with Abundance in Selected Plants of Lamiaceae Family from Vidlic Mountain (Serbia). *Chemosphere* **2011**, *84* (11), 1584–1591. https://doi.org/10.1016/j.chemosphere.2011.05.048.

(91) Harper, A. R.; Santin, C.; Doerr, S. H.; Froyd, C. A.; Albini, D.; Otero, X. L.; Viñas, L.; Pérez-Fernández, B. Chemical Composition of Wildfire Ash Produced in Contrasting Ecosystems and Its Toxicity to Daphnia Magna. *Int J Wildland Fire* **2019**, *28* (10), 726–737. https://doi.org/10.1071/WF18200.

(92) Dimitriadou, S.; Katsanou, K.; Charalabopoulos, S.; Lambrakis, N. Interpretation of the Factors Defining Groundwater Quality of the Site Subjected to Thewildfire of 2007 in Ilia Prefecture, South-Western Greece. *Geosciences (Basel)* **2018**, *8* (4). https://doi.org/10.3390/geosciences8040108.

(93) Rhodes, E. P.; Ren, Z.; Mays, D. C. Zinc Leaching from Tire Crumb Rubber. *Environ Sci Technol* **2012**, *46* (23), 12856–12863. https://doi.org/10.1021/es3024379.

(94) *Scrap Tire Management Council*. http://www.energyjustice.net/files/tires/files/scrapchn.html.

(95) Chen, H.; Awasthi, S. K.; Liu, T.; Duan, Y.; Zhang, Z.; Awasthi, M. K. Compost Biochar Application to Contaminated Soil Reduces the (Im)Mobilization and Phytoavailability of Lead and Copper. *Journal of Chemical Technology and Biotechnology* **2020**, *95* (2), 408–417. https://doi.org/10.1002/jctb.5986.

(96) Wang, X.; Guo, Q.; Wang, X.; Jia, Y.; Chen, W.; Zhang, Q.; Yuan, J. Study on the Effects of New Developed Biochar and Sludge Composite Materials on Copper and Lead Contaminated Soil and

Its Remediation Mechanism. *Environ Technol Innov* **2023**, *32*, 103429. https://doi.org/10.1016/j.eti.2023.103429.

(97) Lopez, A. M.; Pacheco, J. L.; Fendorf, S. Metal Toxin Threat in Wildland Fires Determined by Geology and Fire Severity. *Nat Commun* **2023**, *14* (1), 8007. https://doi.org/10.1038/s41467-023-43101-9.

(98) Rascio, I.; Allegretta, I.; Gattullo, C. E.; Porfido, C.; Suranna, G. P.; Grisorio, R.; Spiers, K. M.; Falkenberg, G.; Terzano, R. Evidence of Hexavalent Chromium Formation and Changes of Cr Speciation after Laboratory-Simulated Fires of Composted Tannery Sludges Long-Term Amended Agricultural Soils. *J Hazard Mater* **2022**, *436* (April), 129117. https://doi.org/10.1016/j.jhazmat.2022.129117.

(99) Burke, M. P.; Hogue, T. S.; Kinoshita, A. M.; Barco, J.; Wessel, C.; Stein, E. D. Pre- and Post-Fire Pollutant Loads in an Urban Fringe Watershed in Southern California. *Environ Monit Assess* **2013**, *185* (12), 10131–10145. https://doi.org/10.1007/s10661-013-3318-9.

(100) Pinedo-Gonzalez, P.; Hellige, B.; West, A. J.; Sañudo-Wilhelmy, S. A. Changes in the Size Partitioning of Metals in Storm Runoff Following Wildfires: Implications for the Transport of Bioactive Trace Metals. *Applied Geochemistry* **2017**, *83*, 62–71. https://doi.org/10.1016/j.apgeochem.2016.07.016.

(101) Drysdale, M.; Bjorklund, K. L.; Jamieson, H. E.; Weinstein, P.; Cook, A.; Watkins, R. T. Evaluating the Respiratory Bioaccessibility of Nickel in Soil through the Use of a Simulated Lung Fluid. *Environ Geochem Health* **2012**, *34* (2), 279–288. https://doi.org/10.1007/s10653-011-9435-x.

(102) Begum, W.; Rai, S.; Banerjee, S.; Bhattacharjee, S.; Mondal, M. H.; Bhattarai, A.; Saha, B. A Comprehensive Review on the Sources, Essentiality and Toxicological Profile of Nickel. *RSC Adv* **2022**, *12* (15), 9139–9153. https://doi.org/10.1039/d2ra00378c.

(103) Gaetke, L. M.; Chow, C. K. Copper Toxicity, Oxidative Stress, and Antioxidant Nutrients. *Toxicology* **2003**, *189* (1–2), 147–163. https://doi.org/10.1016/S0300-483X(03)00159-8.

(104) Twining, J.; McGlinn, P.; Loi, E.; Smith, K.; Gieré, R. Risk Ranking of Bioaccessible Metals from Fly Ash Dissolved in Simulated Lung and Gut Fluids. *Environ Sci Technol* **2005**, *39* (19), 7749–7756. https://doi.org/10.1021/es0502369.

(105) Koleli, N.; Demir, A. *Chromite*; Elsevier Inc., 2016. https://doi.org/10.1016/B978-0-12-803837-6.00011-1.

(106) Levy, D. B.; Barbarick, K. A.; Siemer, E. G.; Sommers, L. E. Distribution and Partitioning of Trace Metals in Contaminated Soils near Leadville, Colorado. *J Environ Qual* **1992**, *21* (2), 185–195. https://doi.org/10.2134/jeq1992.00472425002100020006x.

(107) Ré, A.; Rocha, A. T.; Campos, I.; Marques, S. M.; Keizer, J. J.; Gonçalves, F. J. M.; Pereira, J. L.; Abrantes, N. Impacts of Wildfires in Aquatic Organisms: Biomarker Responses and Erythrocyte Nuclear Abnormalities in Gambusia Holbrooki Exposed in Situ. *Environmental Science and Pollution Research* **2021**, *28* (37), 51733–51744. https://doi.org/10.1007/s11356-021-14377-5.

(108) Twining, J.; McGlinn, P.; Loi, E.; Smith, K.; Gieré, R. Risk Ranking of Bioaccessible Metals from Fly Ash Dissolved in Simulated Lung and Gut Fluids. *Environ Sci Technol* **2005**, *39* (19), 7749–7756. https://doi.org/10.1021/es0502369.